GEOMETRY OF RAPIDLY SOLIDIFIED RIBBONS  
FOR MILITARY APPLICATIONSM.F. Abdel-Ghafar  
N.A. El-Mahallawy and M.A. Taha\*

## ABSTRACT

This work aims to study the influence of processing variables in melt spinning - which is one of the rapid solidification processes (RSP) - on the geometry of the ribbons produced directly from the melt.

The RSP is one of the recent manufacturing techniques, in which the final products - ribbons and fibers - could be produced directly by solidification of liquid alloys, thus saving all further conventional metal forming processes usually carried out.

In this investigation, a melt spinning apparatus was designed and constructed in order to produce ribbons from the melt using a rotating substrate in the form of wheel. The alloys studied were aluminium alloys with 0, 5.23, 13.46 and 33 wt% Cu.

The processing variables used were as follows: substrate linear velocity ( $v$ ) ranging from 2 to 20  $\text{m.s}^{-1}$ , injection pressure of the melt ( $P$ ) ranging from  $2.9 \times 10^4$  to  $6.8 \times 10^4 \text{ N.m}^{-2}$ , substrate thermal conductivity ( $K$ ) ranging from 43.3 to  $386.6 \text{ W.m}^{-1}.\text{K}^{-1}$ , melt superheating temperature ( $\Delta T$ ) ranging from 0 to 150 K, nozzle - substrate distance ( $H$ ) ranging from 5 to 20 mm and nozzle diameter ( $d$ ) ranging from 0.5 to 2 mm. The geometry of the product; ribbon thickness ( $t$ ), width ( $w$ ), length ( $L$ ) and surface roughness ( $R_t$ ) have been measured and they were correlated with the different processing variables.

It is found that  $v$  plays the most important role in determining the geometry parameters, where a critical velocity of  $5 \text{ m.s}^{-1}$  is found. Varying  $v$  up to this value causes increase in  $w$  and  $L$  and a decrease in  $t$ . Increasing  $v$  beyond this value causes decrease in  $w$ ,  $L$  and  $t$ .

---

\* Department of Design and Production Engineering,  
Faculty of Engineering, Ain-Shams University, Abbaseia, Cairo.

The RSP is one of the recent manufacturing techniques, in which the final products - ribbons and fibers - could be produced directly by solidification of liquid alloys, thus saving all further conventional metal forming processes usually carried out.

RSP products differ from powders to continuous sheets. However, great attention is paid to powders and fibres produced by RSP techniques. Many of the jet atomization processes and chill methods have been in existence for some time on a production basis. Some examples of possible RSP products applications for military are:

One of the most important applications of the RSP is the use of powders made by atomization techniques for producing the Rapid Solidified Rate (RSR) Wafer blade [1, 2], which is used in turbine rotors.

The pressed compacts of cast-fibres are stronger than powder compacts, especially when made of a strong ductile material. Such compacts will hold their shapes easily at 10% density, and will not fall apart under shock or load. Under such sever conditions, fibre compact shows little or no damage [3]. Therefore, it is probable that rolled sheets of compacted continuous aluminium fibres could readily replace lead sheets as vibrational energy absorbers, and be lighter and cheaper as well. It is also probable that such fibre sheeting would maintain its damping property over a wide range of temperatures, a performance which very few other damping materials can match. Felts and filters are, of course, other uses to which fibre compacts can be put [3].

An untested market for fibre sheeting is in armour. To defeat an incoming projectile, it is necessary not only to stop the forward movement of the projectile, but to absorb the shockwave produced in the armour itself by the impact before it can produce a spall from the opposite surface. The high damping fibre compacts may excell at this application [3, 4].

A specialized market for continuous cast aluminium fibre of controlled length is as radar chaff [3]. To defeat enemy radar detection, metallic dipoles (i.e., controlled-length fibres) are dispersed from an aircraft. So, it seems feasible to develop an airborne fibre-casting unit (as a chill-block melt spinning unit) capable of dispersing large quantities of dipoles of a length and cross section selected by the pilot and/or control system. Such a system could be used to detect the particular radar being used and has obvious millitary utility.

## EXPERIMENTAL PROCEDURE

In the melt spinning process, a mass is solidified continuously in a ribbon form by a rotating chill-block substrate from a pool of liquid metal or alloy falling on the substrate. In the designed apparatus, the molten metal is pushed using inert gas, through a small orifice. The metal stream falls on a rotating metallic pulley, thus forming a ribbon. Fig.(1).

Al-Cu alloys Al-pure, 5.7-13.33 wt% Cu were prepared from high purity 99.99% aluminium (german grade) and electrolytic copper using a 1 Kg capacity high purity graphite crucible. The molten metal free surface was covered using a continuous flow of nitrogen. The alloys

Al-Cu charges in the form of 50 gms rods were fed into the melt spinning apparatus which was already in operation (i.e. with hot crucible). Usually, this amount of alloy is enough to produce relatively big amount of melt spun ribbons or fibres. After complete melting, the alloy was heated to the desired superheat, then the furnace power was cut off. While the substrate was rotating, the liquid alloy was pushed to fall directly on it. The ribbons formed are collected in front of the apparatus. After each experiment, the pulley was cleaned while it was repolished using a standard silicon carbide paper of 1000 grid size after each 10 experiments.

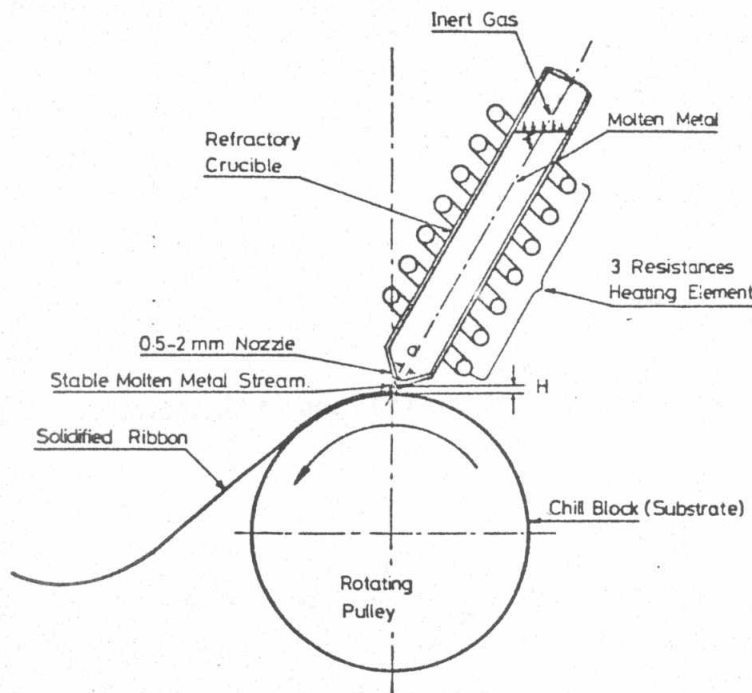


Fig. (1) A schematic diagram showing the melt spinning apparatus.

Influence of v

The influence of v on ribbon average thickness (t), ribbon average width (w) and ribbon maximum fragmentation length (L) is given in fig. (2) a,b and c respectively.

By replotting the results on log-log scale, as shown in fig. (3), a straight line relationship between t and v is obtained with the form of:

$$t = t_0 \cdot v^{-m} \quad \dots\dots\dots 1)$$

This result is in satisfactory agreement with the previous results of Vincent [5], Kavesh [6], Hillmann [7] and El-Mahallawy [8].

It is clear that the exponent m depends on the alloy system (base metal)

On the other hand, the constant t<sub>0</sub> differs with changing the alloy composition

Taking into consideration that Vincent et al. [5] have given a relationship, based on a thermodynamic conditions combined with other previous empirical relations between v and t, in the form of:

$$t \propto Q_r^{0.42} \cdot v^{-0.84} \quad \dots\dots\dots 2)$$

where:

- t = ribbon average thickness.
- Q<sub>r</sub> = metal flow rate = t.w.v.
- v = substrate linear velocity.
- w = ribbon average width.

It can be said that:

$$t = c \cdot Q_r^n \cdot v^{-m} \quad \dots\dots\dots 3)$$

where c is a constant. Comparing equations (3.1) and (3.3), therefore:

$$t_0 = c \cdot Q_r^n \quad \dots\dots\dots 4)$$

This means that the constant t<sub>0</sub> depends on the metal flow rate Q<sub>r</sub>. The other factors such as alloy composition are included in the constant c. Fig. (2 -b) shows that (w) greatly depends on (v). An instability region exists for velocities lower than about 6 m.s<sup>-1</sup>, in which ribbon width increases rapidly with increasing v. This instability region was also reported by Vincent et al. [5] who indicated that it is common for alloys having high surface tension, cast at very low substrate velocities

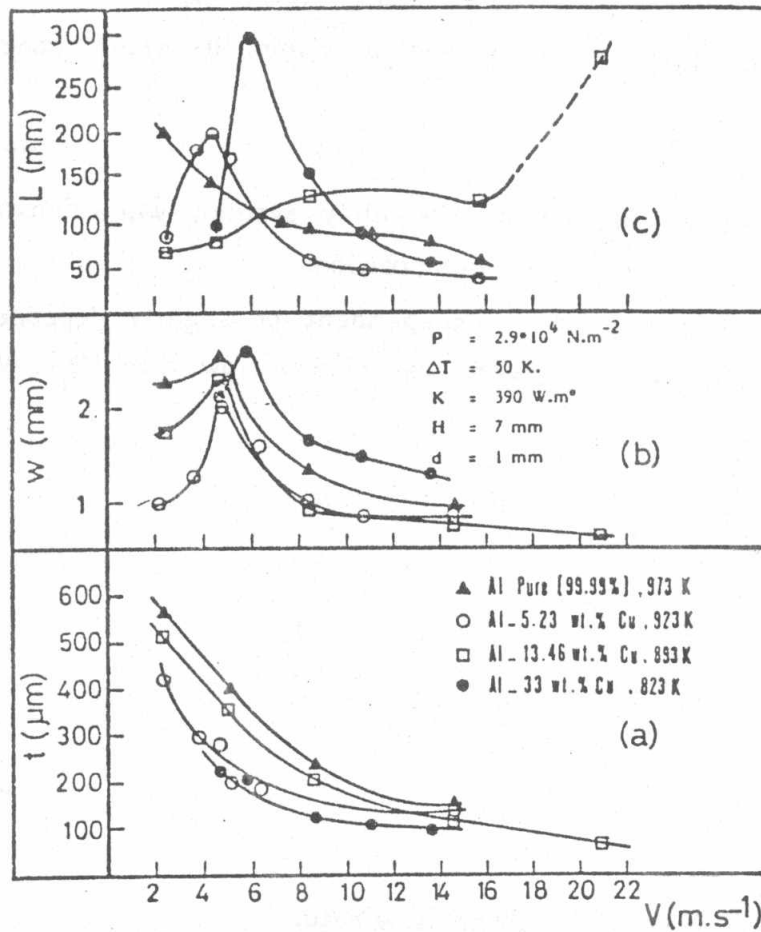


Fig. ( 2 ) Influence of substrate linear velocity (v) on ribbon geometry (t, w & L) and cross sectional shape.

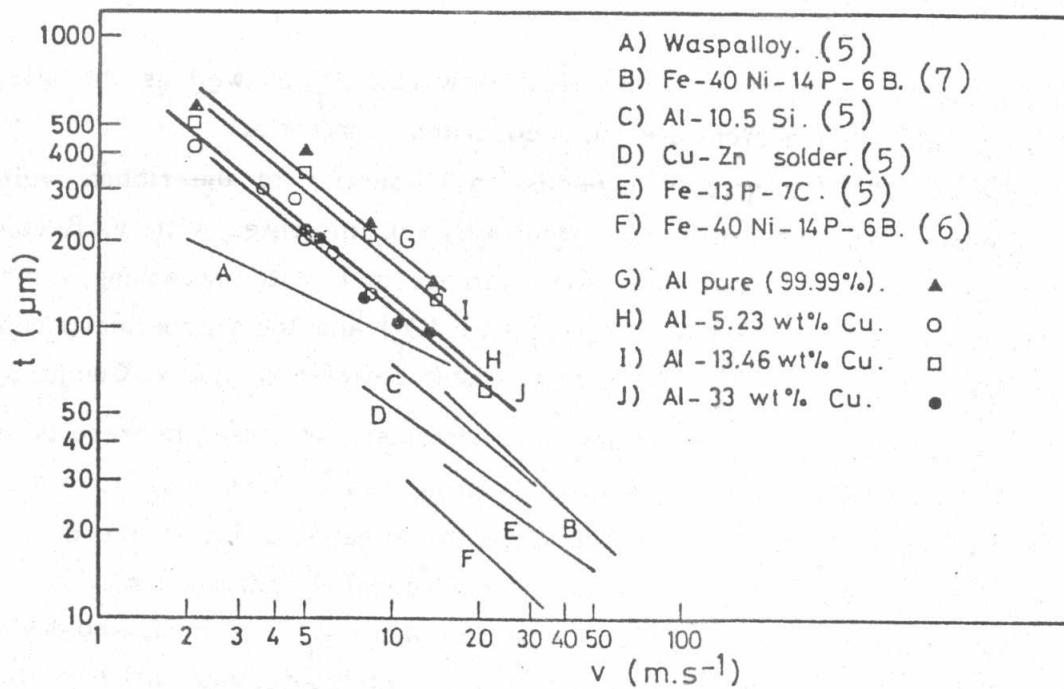


Fig. ( 3 ) Variation of ribbon average thickness (t) with substrate linear velocity (v).

Plotting the present results on a log-log scale, fig. (4), the following relationship between  $v$  and  $w$  within the stable conditions is found:

$$w = w_0 \cdot v^{-q} \quad \dots\dots\dots 5)$$

it is clear that exponent  $q$  depends on the alloy system, while constant  $w_0$  differs according to the alloy composition.

It was found previously that  $w$  is independent or slightly dependent on  $v$ , but strongly dependent on the theoretical ribbon flow rate ( $Q_r$ ). Vincent et al. [5] found that:

$$w \propto Q_r^p \cdot v^{-q} \quad \dots\dots\dots 6)$$

i.e.  $w = a \cdot Q_r^p \cdot v^{-q} \quad \dots\dots\dots 7)$

From equations (3.5) and (3.7),

$$w_0 = a \cdot Q_r^p \quad \dots\dots\dots 8)$$

where:

$Q_r$  = t.w.v = theoretical ribbon flow rate.

$a$  = constant.

$p$  and  $q$  = exponents.

This means that  $w_0$  depends on the metal flow rate  $Q_r$  as well as the alloy composition, while other factors are included in the constant  $a$ .

Fig. 2c indicates that ( $L$ ) greatly depends on  $v$ , similar to the ribbon width ( $w$ ). A similar instability region is found where  $L$  increases with  $v$ . Beyond a critical value of  $v$ ,  $L$  decreases. The decrease in  $L$  with increasing  $v$  may be due to the difference between pouring rate ( $Q_p$ ) and the theoretical ribbon flow rate ( $Q_r$ ). Fig. (5) indicates the relationship between  $Q_r$  and  $v$ . Comparing fig. (2-c) with fig. (5) and taking into consideration that the results in fig. (2-c) are obtained by using small pouring rates, it is easy to notice that both figures emphasize that the fragmentation happens due to the difference between  $Q_p$  and  $Q_r$  and is not a mechanical fragmentation. This is more indicated for the alloy Al-13.46 wt% Cu where  $Q_p$  was measured ( $1450 \text{ mm}^3 \cdot \text{s}^{-1}$ ). This value is plotted in fig. (5) as a horizontal line since it was constant for the considered set of experiments. As the figure shows, this

line divided the curve for  $Q_r$ - $v$  relationship into two regions: region of ribbon fragmentation where a part of the curve exists above the line ( $Q_r > Q_p$ ) and a region of ribbon continuity where the curve exists below the line ( $Q_r < Q_p$ ). However, as the curve is lower than the  $Q_p$  line, the ribbon becomes non-uniform with thick nodes.

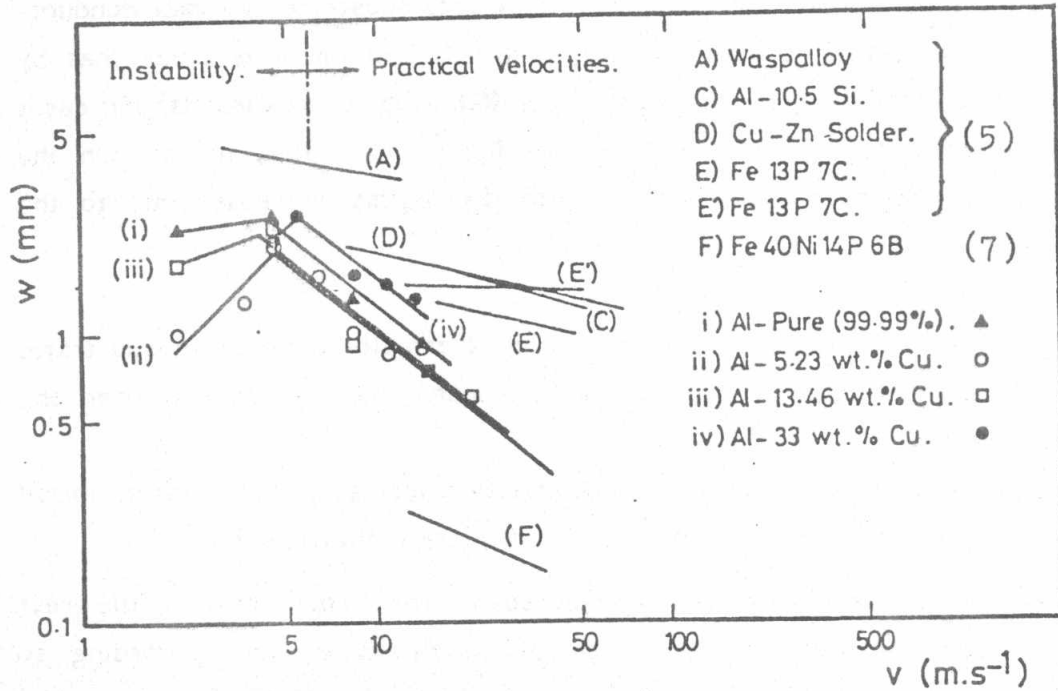


Fig. ( 4 ) Influence of substrate linear velocity ( $v$ ) on ribbon average width ( $w$ ).

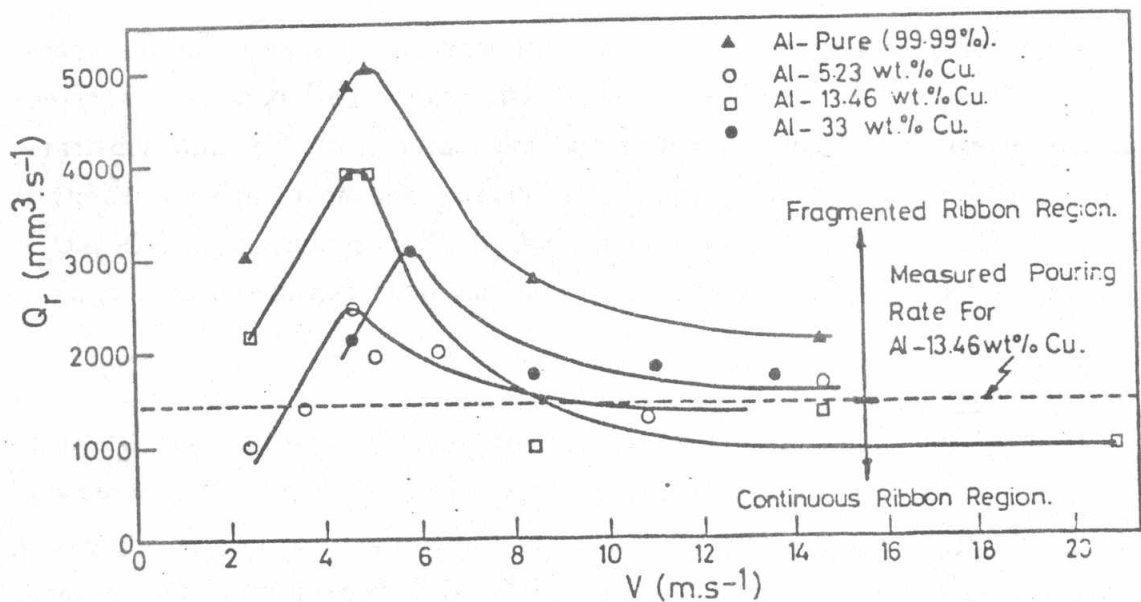


Fig.( 5 ) Variation of theoretical ribbon flow rate( $Q_r$ ) with substrate linear velocity ( $v$ ).

### Influence of substrate material

Substrate material affects mainly ribbon formation due to its thermal properties since it acts as a heat sink which cools the molten metal into the form of ribbon. Three different materials were used in the present work as substrates; steel, brass and copper. Influence of substrate thermal conductivity ( $K$ ) on  $t, w$  and  $L$  is shown in fig. ( 6 a,b and c). It is clear that by increasing the substrate thermal conductivity ( $K$ ), ribbon thickness ( $t$ ) increases while its width ( $w$ ) decreases with a rate higher than that of  $t$ . On the other hand, maximum fragmentation length ( $L$ ) rapidly increases due to the increase of  $K$ .

When the molten metal impacts a high thermally conductive substrate, it solidifies so fast that it, does not find enough time to spread over the substrate surface,

Vice versa, using a low thermal conductivity substrate, the molten metal finds longer time to spread before its complete solidification

After solidification had been completed in the cross section, the rest of molten metal spreads in the longitudinal direction, and according to the difference between the pouring rate ( $Q_p$ ) and theoretical ribbon flow rate ( $Q_r$ ), fragmentation happens.

Kavesh [6] had reported a similar influence of substrate thermal conductivity ( $K$ ) on ribbon average thickness ( $t$ ). kavesh [6.] had also reported that, the appropriate figure of merit for the material of the chill substrate is the product of its thermal conductivity, density and heat capacity ( $K \cdot \rho \cdot C_p$ ) rather than its thermal diffusivity ( $K / (\rho \cdot C_p)$ ). Copper has higher ( $K \cdot \rho \cdot C_p$ ) product than other metals and indeed copper has been considered as a typical chill substrate.

### Influence of P

Fig. ( 7 -a,b and c) shows the influence of injection gas pressure ( $P$ ) on  $t, w$  and  $L$ . The figure shows that  $t, w$  and  $L$  increase with increasing  $P$ . It is a logical result because when the injection pressure is increased, the pouring rate ( $Q_p$ ) will increase. Fig. ( 7 -a) indicates that if  $P$  is more than about  $4.9 \times 10^4 \text{ N.m}^{-2}$  ( $0.5 \text{ Kg.cm}^{-2}$ ), ribbon average thickness ( $t$ ) will

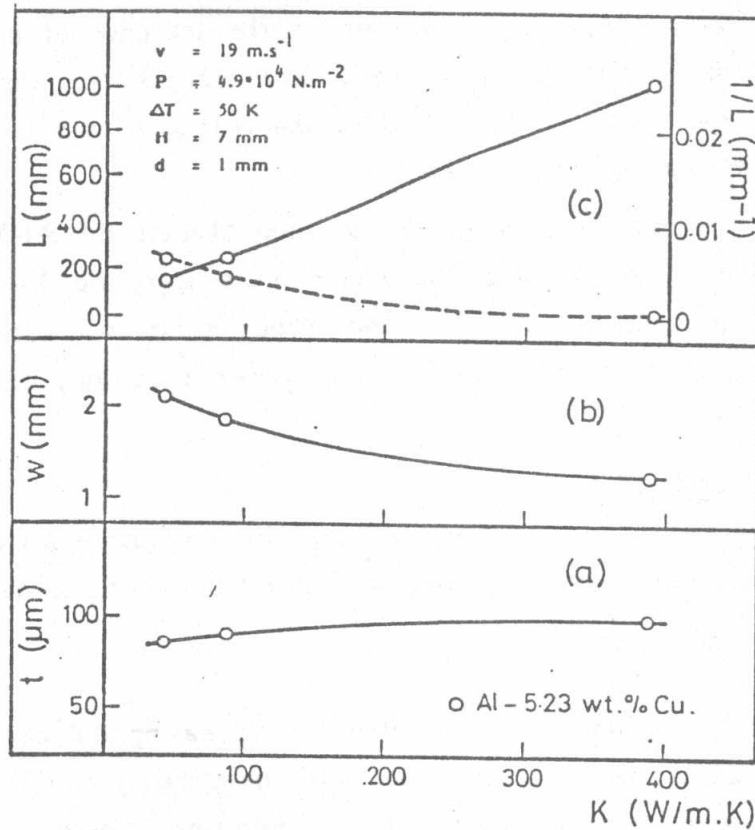


Fig. ( 6 ) Influence of substrate thermal conductivity on ribbon geometry and cross sectional shape

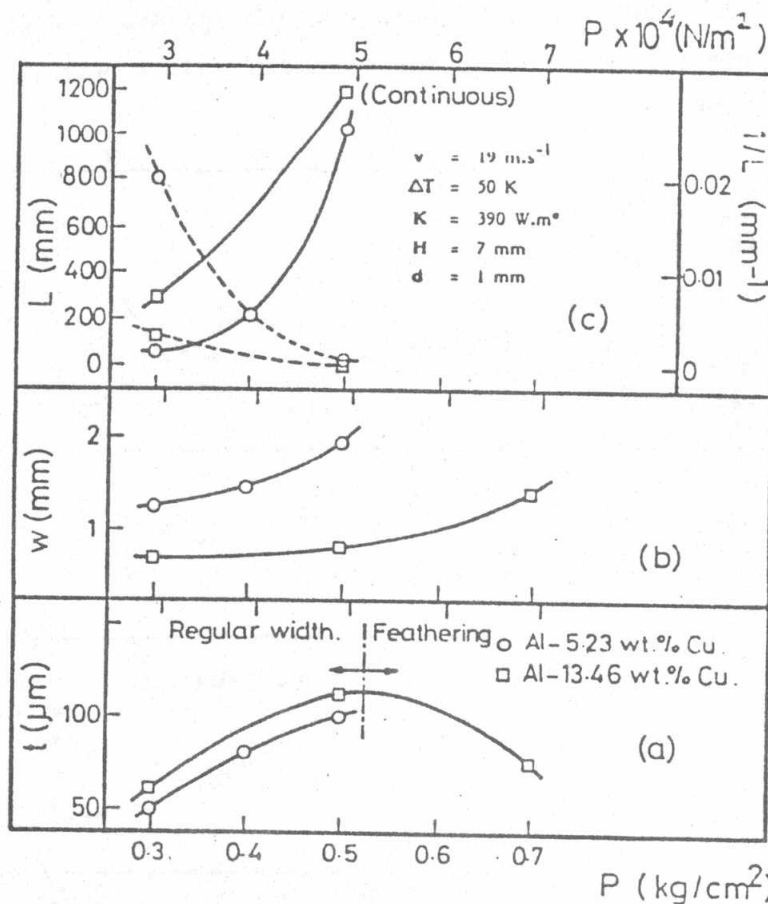


Fig. ( 7 ) Influence of injection gas pressure (P) on ribbon geometry (t,w & L) and cross sectional shape.

decrease. This is believed to be due to the increase of impact force which tends to reduce the ribbon thickness and spreads the molten metal in the width direction. Often, this is accompanied with width irregularity which results in ribbon with feathering.

It is noticed in fig. (7 -a,b and c) that the Al-5.23 wt% Cu alloy tends to spread in the width direction more than the Al-13.46 wt% Cu and vice versa in case of the thickness direction. It is unexpected result since the Al-5.23 wt% Cu alloy has fluidity lower than that of the Al-13.46 wt% Cu alloy.

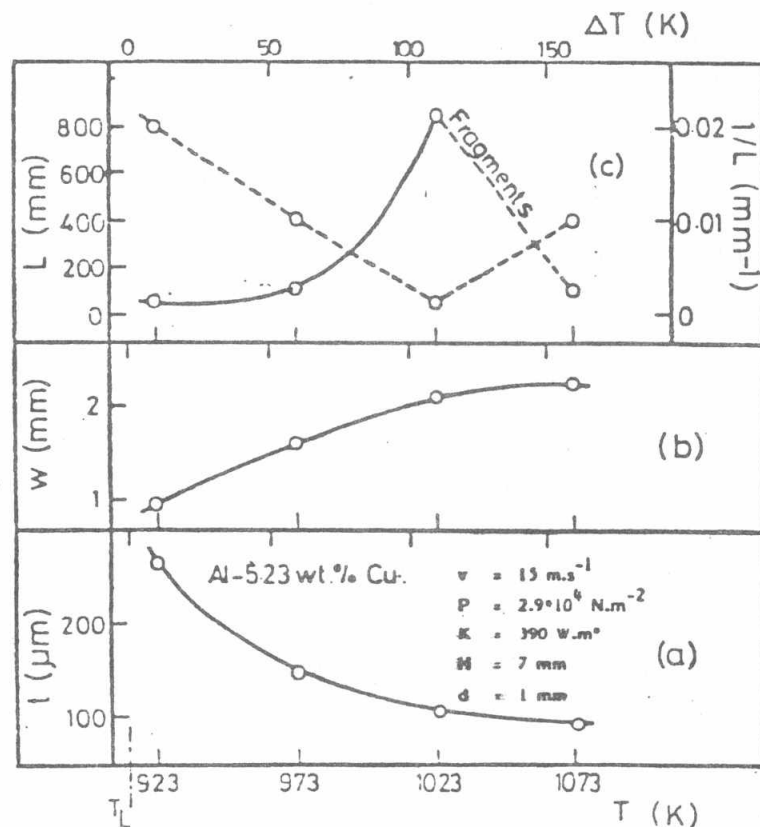
#### Influence of $\Delta T$

Fig. (8 -a,b and c) shows that by increasing  $\Delta T$ ,  $t$  decreases while  $w$  and  $L$  increases up to a value of  $\Delta T = 150$  K. This is due to the increase of molten metal fluidity.

Fig. (8 -a,b and c) shows that by increasing  $\Delta T$  above  $\Delta T = 150$  K,  $t$  still decreases, while  $w$  increases with irregularity and  $L$  rapidly decreases so that a form of small shots and nonsolidified splashes are produced. This change in behaviour is due to the high  $\Delta T$  that the substrate is no longer able to solidify the melt completely on its surface. As a result, a stream of molten metal droplets leave the substrate surface with a resultant force given by:

$$\bar{R} = \sqrt{\bar{F}_t^2 + (\bar{F}_d - \bar{F}_l)^2}$$

Fig (8) Influence of melt temperature ( $T$ ) and melt superheat ( $\Delta T$ ) on ribbon geometry and cross sectional shape.



where:

- $F_t$  = tangential force due to substrate rotational velocity.  
 $F_c$  = centrifugal force due to substrate rotational velocity.  
 $F_I$  = impacting force of the molten metal stream at point of its contact with the substrate surface due to the injection pressure.

#### Influence of H on t:

Fig. ( 9 ) illustrates the variations of ribbon average thickness ( $t$ ) with nozzle-substrate distance ( $H$ ). It shows that  $t$  increases with increasing  $H$ . This increase of  $t$  is accompanied with higher scattering in  $t$  values, which means that the molten metal flow through the nozzle-substrate distance changes into turbulent flow above  $H$  equals about 12 mm. The increase in  $t$  may be due to the partial solidification of the molten metal taking place within the nozzle-substrate distance. This partial solidification happens only when  $H$  is large enough. That explains the reason of the rapid increase in  $t$  for  $H > 12$  mm nearly.

Fig. ( 10 ) illustrates the variation of ribbon average width ( $w$ ) with nozzle-substrate distance ( $H$ ). It shows that by increasing of  $H$ ,  $w$  increases. At the same time, the scatter in the width values increases. From the experimental work, it was noticed that by increasing  $H$ , the impact of the molten metal on the substrate surface increases causing splashing and feathering defects in the ribbon.

Fig. ( 11 ) illustrates the variation of the maximum fragmentation length ( $L$ ) with nozzle-substrate distance ( $H$ ). It shows that  $L$  increases with increasing  $H$  up to a value of  $H = 15$  mm after which  $L$  decreases. That may be due to the resultant forces of both impact and tangential forces which increase causing ribbon fragmentation into flakes. These results were obtained at substrate linear velocity ( $v$ ) equals  $6 \text{ m.s}^{-1}$ , another result in the same figure using  $v = 15 \text{ m.s}^{-1}$  shows that due to the increase of  $v$ , slope of the curve increased and the critical point (beginning of fragmentation) shifted to  $H = 10$  mm. However, most of previous investigators used  $H$  ranging between 1 and 8 mm [9, 10, 11, 12] Huang and Fiedler [13] used  $H = 0.25$  mm for plainer flow casting of ribbons as a special case to study the ribbon roughness.

Fig. (9.) Influence of nozzle-substrate distance (H) on ribbon average thickness (t).

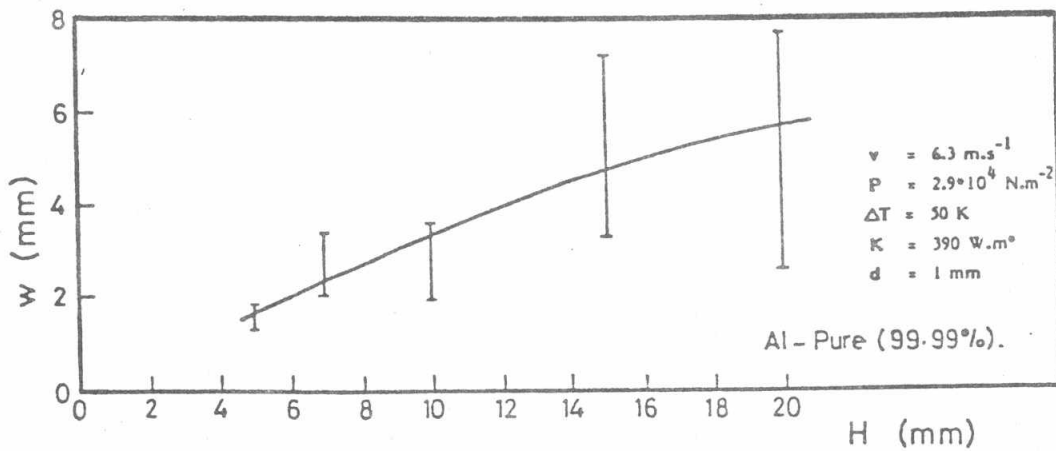
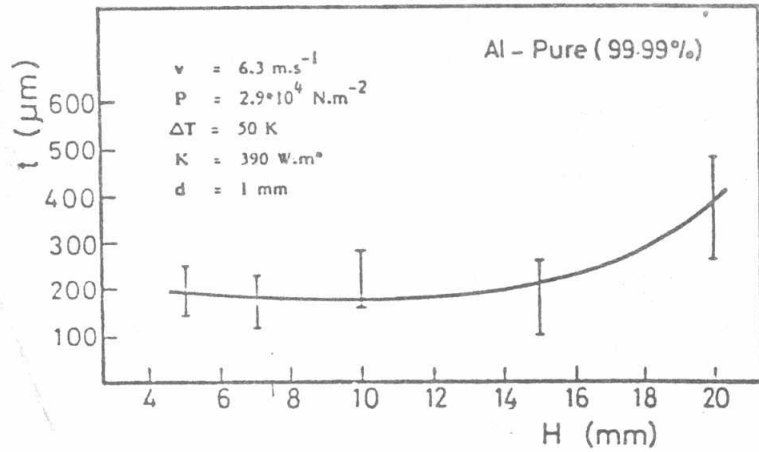


Fig. (10) Influence of nozzle-substrate distance (H) on ribbon average width (w).

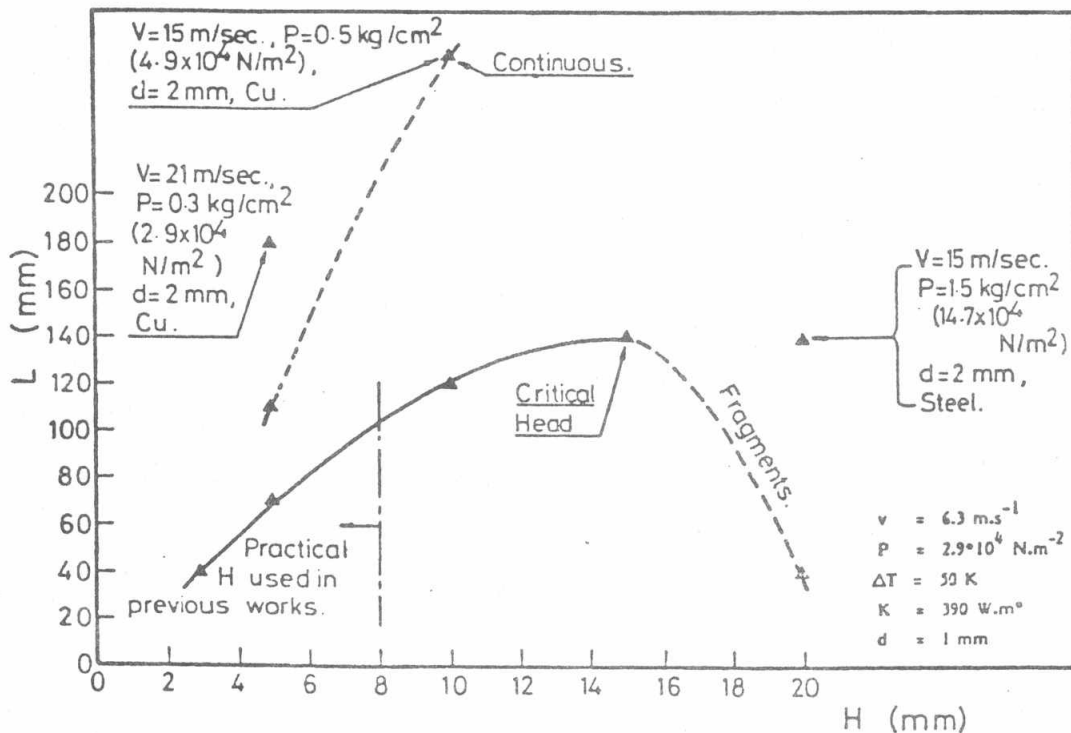


Fig. (11) Influence of nozzle-substrate distance (H) on ribbon maximum fragmentation length (L).

Influence of nozzle diameter (d)

Fig. ( 12 ) shows the effect of using different nozzle diameters (d) of 1 and 1.5 mm. The results show that by increasing the nozzle diameter, ribbon average width (w) increases and tendency to form "feathering" is enhanced. Also by increasing d, maximum fragmentation length (L) increases and ribbon average thickness (t) decreases. Normally, nozzle diameter ranging between 0.5 and 1.5 mm are used. when using larger diameter, the molten metal flow through the nozzle was unstable which resulted in irregularities in both thickness and width (feathering in the case of width), and consequently irregularities in the maximum fragmentation length too.

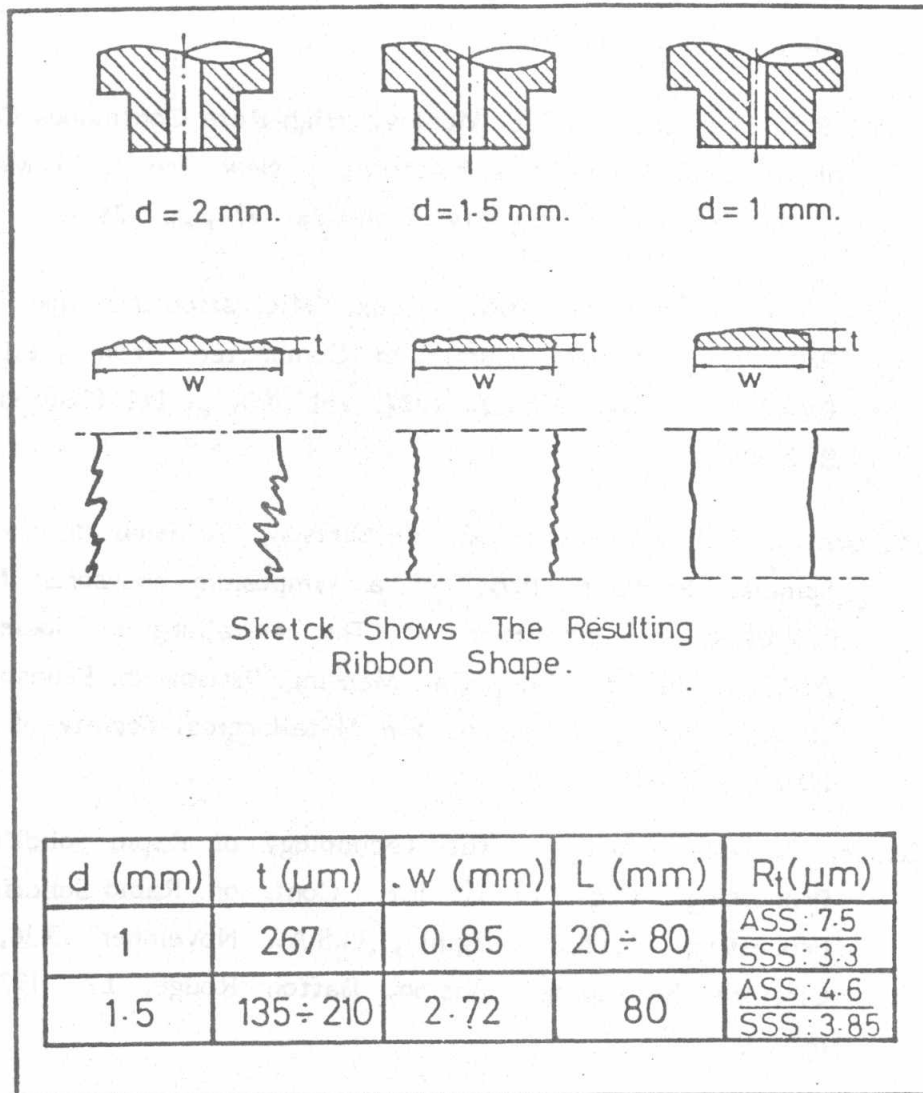


Fig. ( 12 ) Influence of nozzle diameter (d) on ribbon geometry

REFERENCES

1. R.E. Anderson, A.R. Cox, T.D. Tillman and E.C. Van Reuth, E.C. Van Reuth, "Use of RSR Alloys for High Performance Turbine Airfoils", Proc. of 2nd Int. Conf. on Rapid Solidification Processing, Reston, Virginia, U.S.A., March 23-26, 1980, Claitor's Publishing Division, Baton Rouge, LA., 1980, pp. 416-28.
2. A.L. Bement and E.C. Van Reuth, "Quo Vadis-RSR", Proc. 2nd Int. Conf. on Rapid Solidification Processing, Reston, Virginia, U.S.A. March 23-26, 1980, Claitor's Publishing Division, Baton Rouge, LA., 1980, pp. 404-15.
3. R.B. Pond, R.E. Maringer and C.E. Mobley, "High-Rate Continuous Casting of Metallic Fibres and Filaments", New Trends in Material Processing, ed. Am. Society of Metals, 1974, pp. 128-46.
4. C.E. Mobley, A.H. Clauer and B.A. Wilcox, "Microstructures and Tensile Properties of 7075 Aluminium Compacted from Melt-Spun Ribbon", J. Inst. Metals, 1972, vol. 100, p. 142 (Quoted from Ref. 49).
5. J.H. Vincent, H.A. Davies and J.G. Herbertson, "A Study of the Melt Spinning Process", Proc. of a symposium sponsored by the Solidification Committee of The Metallurgical Society of AIME at the TMS-AIME Fall Meeting, Pittsburgh, Pennsylvania, Oct. 8, 1980. Published by the Metallurgical Society of AIME, 1980, pp. 103-16.
6. S. Kavesh, "Metallic Glasses - The Technology of Rapid Solidification Processing", Proc. of 1st Int. Conf. on Rapid Solidification Processing, Reston, Virginia, U.S.A., November 13-16, 1977, Claitor's Publishing Division, Baton Rouge, LA, 1977, pp. 165-87.
7. H. Hillman and H.R. Hilzinger, Proc. 3rd Int. Conf. on Rapidly quenched Metals, Brighton, July 1978, ed. B. Cantor, Published by Metals Society, London, 1978, vol. 1, pp. 22-29. (Quoted from Ref. 51).

8. N.A. El-Mahallawy and M.A. Taha, "Simulations and Experiments in Pressurised Solidification Process (PSP) and Rapid Solidification Process (RSP)", Paper published in The Engineering Foundation Conf. for Modeling of Casting and Welding Processes held at New England College, Henniker, New Hampshire, July 31-August 5, 1983.
9. W. Hug, "Nucleation in Rapidly Solidifying Ribbons", Topics on Nucleation-Rapid Solidification held at the Foundry Institute, The Technical University of Aachen, W. Germany, 14/15 March 1983, pp. 34-53.
10. Uwe Köster, Ursula Herold and Hans-Georg Hillenbrand, "Influence of Solidification Parameters on Mechanical Properties and Thermal Stability of Fe-Ni-B Metallic Glasses", Paper published in Materials Research Society Annual Meeting, Boston, 16-19 November 1981.
11. J.V. Wood, "Rapid Casting of Metallic Wires", Proc. Int. Conf. on Solidification held at the Univ. of Sheffield on 18-21 July 1977, pp. 496-500.
12. A. Handasayde Dicke, M.C. Simms, D.D. Double and A. Hellawell, "Sheet Casting Process for Aluminium and Aluminium Alloys", Proc. Int. Conf. on Solidification held at the University of Sheffield on 18-21 July 1977, pp. 486-9.
13. S.C. Huang and H.C. Fiedler, "Effects of Wheel Surface Finish and Wheel Speed on the Topography of Amorphous Ribbons", Proc. of symposium sponsored by The Solidification Committee of The Metallurgical Society of AIME at The TMS-AIME Fall Meeting, Pittsburgh, Pennsylvania, Oct. 8, 1980, Published by The Metallurgical Society of AIME, 1980, pp. 225-31.